2024-03

DETECTION PERFORMANCE EVALUATION IN SPACE-TIME ADAPTIVE PROCESSING USING ENHANCED ELECTRONIC PROTECTION MITIGATION AGAINST ADVANCED SHAPED INTERFERENCE

Lee, Wee Keong I.

Monterey, CA; Naval Postgraduate School

NAVAL POSTGRADUATE SCHOOL

MONTEREY, CALIFORNIA

THESIS

DETECTION PERFORMANCE EVALUATION IN SPACE-TIME ADAPTIVE PROCESSING USING ENHANCED ELECTRONIC PROTECTION MITIGATION AGAINST ADVANCED SHAPED INTERFERENCES

by

Wee Keong I. Lee

March 2024

Thesis Advisor: Ric Romero
Second Reader: David C. Jenn

THIS PAGE INTENTIONALLY LEFT BLANK

REPORT DOCUMENTATION PAGE			*Form Approved OMB No. 0704-0188*

1. AGENCY USE ONLY *(Leave blank)*	**2. REPORT DATE** March 2024	**3. REPORT TYPE AND DATES COVERED** Master's thesis

4. TITLE AND SUBTITLE DETECTION PERFORMANCE EVALUATION IN SPACE-TIME ADAPTIVE PROCESSING USING ENHANCED ELECTRONIC PROTECTION MITIGATION AGAINST ADVANCED SHAPED INTERFERENCES	**5. FUNDING NUMBERS**
6. AUTHOR(S) Wee Keong I. Lee	
7. PERFORMING ORGANIZATION NAME(S) AND ADDRESS(ES) Naval Postgraduate School Monterey, CA 93943-5000	**8. PERFORMING ORGANIZATION REPORT NUMBER**
9. SPONSORING / MONITORING AGENCY NAME(S) AND ADDRESS(ES) N/A	**10. SPONSORING / MONITORING AGENCY REPORT NUMBER**

11. SUPPLEMENTARY NOTES The views expressed in this thesis are those of the author and do not reflect the official policy or position of the Department of Defense or the U.S. Government.

12a. DISTRIBUTION / AVAILABILITY STATEMENT Approved for public release. Distribution is unlimited.	**12b. DISTRIBUTION CODE** A

13. ABSTRACT (maximum 200 words)

This paper introduces the formulation of the transmit-waveform-shaped noise jammer (TWS-NJ) as an electronic attack (EA) or noise interference method into space-time adaptive processing (STAP). Monte Carlo simulation reveals a substantial impact on target detection, particularly when the TWS-NJ is co-located with the target in the same spatial cell. Comparative analyses against conventional noise interference like the broadband noise jammer (BB-NJ) underline the superior performance of the TWS-NJ in degrading target detection, especially in the absence of electronic protection (EP) implementation. The study highlights the significance of considering both waveform characteristics and spatial locations of noise interferences when assessing their impact on detection performance. Moreover, the study demonstrates that with electronic support (ES) and an accurate noise interference covariance matrix estimate, the generalized matched filter (GMF) emerges as a highly effective STAP EP technique for mitigating adaptive shaped interference.

14. SUBJECT TERMS signal processing, STAP, electronic warfare	**15. NUMBER OF PAGES** 61
	16. PRICE CODE

17. SECURITY CLASSIFICATION OF REPORT Unclassified	**18. SECURITY CLASSIFICATION OF THIS PAGE** Unclassified	**19. SECURITY CLASSIFICATION OF ABSTRACT** Unclassified	**20. LIMITATION OF ABSTRACT** UU

NSN 7540-01-280-5500

Standard Form 298 (Rev. 2-89)
Prescribed by ANSI Std. 239-18

THIS PAGE INTENTIONALLY LEFT BLANK

Approved for public release. Distribution is unlimited.

DETECTION PERFORMANCE EVALUATION IN SPACE-TIME ADAPTIVE PROCESSING USING ENHANCED ELECTRONIC PROTECTION MITIGATION AGAINST ADVANCED SHAPED INTERFERENCES

Wee Keong I. Lee
Military Expert 5, Republic of Singapore Navy
BE, Nanyang Technological University, 2010

Submitted in partial fulfillment of the
requirements for the degree of

**MASTER OF SCIENCE IN ENGINEERING SCIENCE
(ELECTRICAL ENGINEERING)**

from the

**NAVAL POSTGRADUATE SCHOOL
March 2024**

Approved by: Ric Romero
Advisor

David C. Jenn
Second Reader

Douglas J. Fouts
Chair, Department of Electrical and Computer Engineering

THIS PAGE INTENTIONALLY LEFT BLANK

ABSTRACT

This paper introduces the formulation of the transmit-waveform-shaped noise jammer (TWS-NJ) as an electronic attack (EA) or noise interference method into space-time adaptive processing (STAP). Monte Carlo simulation reveals a substantial impact on target detection, particularly when the TWS-NJ is co-located with the target in the same spatial cell. Comparative analyses against conventional noise interference like the broadband noise jammer (BB-NJ) underline the superior performance of the TWS-NJ in degrading target detection, especially in the absence of electronic protection (EP) implementation. The study highlights the significance of considering both waveform characteristics and spatial locations of noise interferences when assessing their impact on detection performance. Moreover, the study demonstrates that with electronic support (ES) and an accurate noise interference covariance matrix estimate, the generalized matched filter (GMF) emerges as a highly effective STAP EP technique for mitigating adaptive shaped interference.

THIS PAGE INTENTIONALLY LEFT BLANK

Table of Contents

List of Figures

List of Acronyms and Abbreviations

AWGN	additive white Gaussian noise
BB-NJ	broadband noise jammer
CNR	clutter-to-noise ratio
CPI	coherent processing interval
DRFM	digital RF memory
EA	electronic attack
ECCM	electronic counter-countermeasure
EP	electronic protection
ES	electronic support
ESD	energy spectral density
GMF	generalized matched filter
JNR	jammer-to-noise ratio
MC	Monte Carlo
MTI	moving target indicator
P_D	probability of detection
P_{FA}	probability of false alarm
PSD	power spectral density
SINR	signal-to-interference noise ratio
SNR	signal-to-noise ratio

STAP space time adaptive processing

TWS-NJ transmit-waveform-shaped noise interference or jammer

TWS transmit-waveform-shaped

CHAPTER 1:
Introduction

Modern defense systems have undergone a paradigm shift, transforming the nature of battles from face-to-face confrontations on open seas to more complex scenarios. In this evolving landscape, aircraft are equipped with advanced radar technologies and play a crucial role for target surveillance, tracking, and targeting. One such technology illustrated in Fig. 1.1 is the moving target indicator (MTI) radar, which leverages space-time adaptive processing (STAP) to integrate joint temporal and spatial filtering and enhances detection capabilities. In the illustration, $\mathbf{k}(\phi, \theta)$ is a unit vector pointing normal to the plane wave, ϕ and θ denotes the azimuth and depression angles [1].

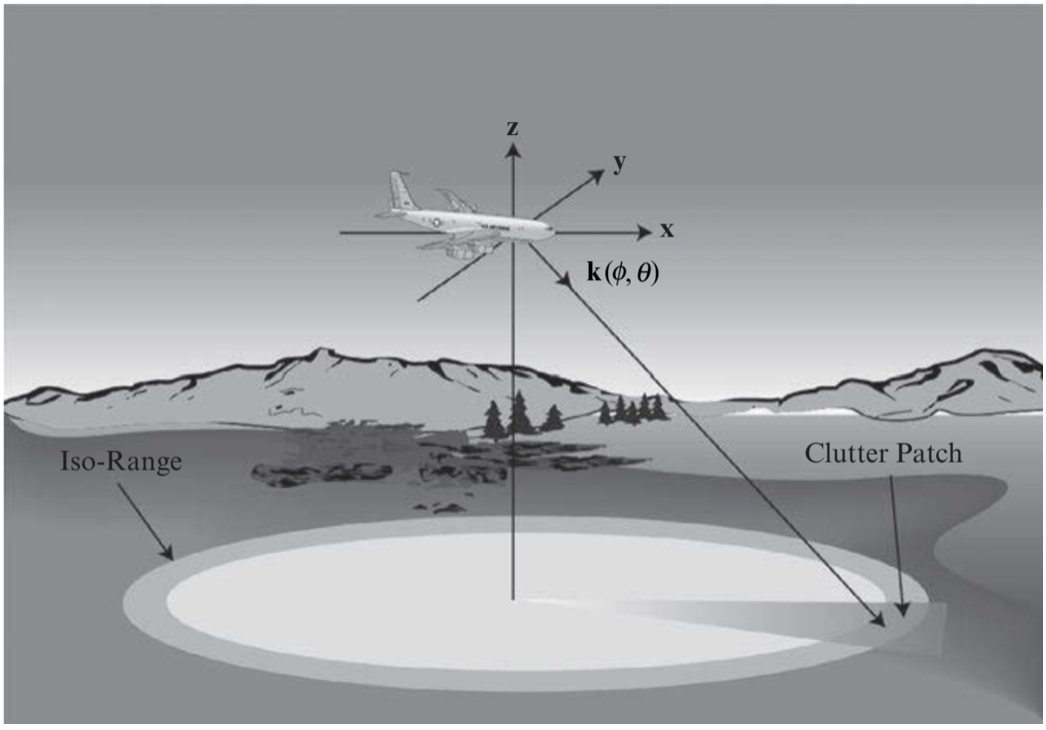

Figure 1.1. MTI radar leverages on STAP to compute clutter returns. Source: [1]

In tandem with the rapid evolution of radar and sensing technologies, adversaries are strategically advancing their electronic warfare (EW) capabilities to exploit vulnerabilities and evade detection. This perpetual cat-and-mouse game is unfolding in the expansive and dynamic battleground of the electromagnetic spectrum, as depicted in Fig. 1.2 [2]. This spectrum serves as the arena where modern military operations are intricately interwoven with electronic activities.

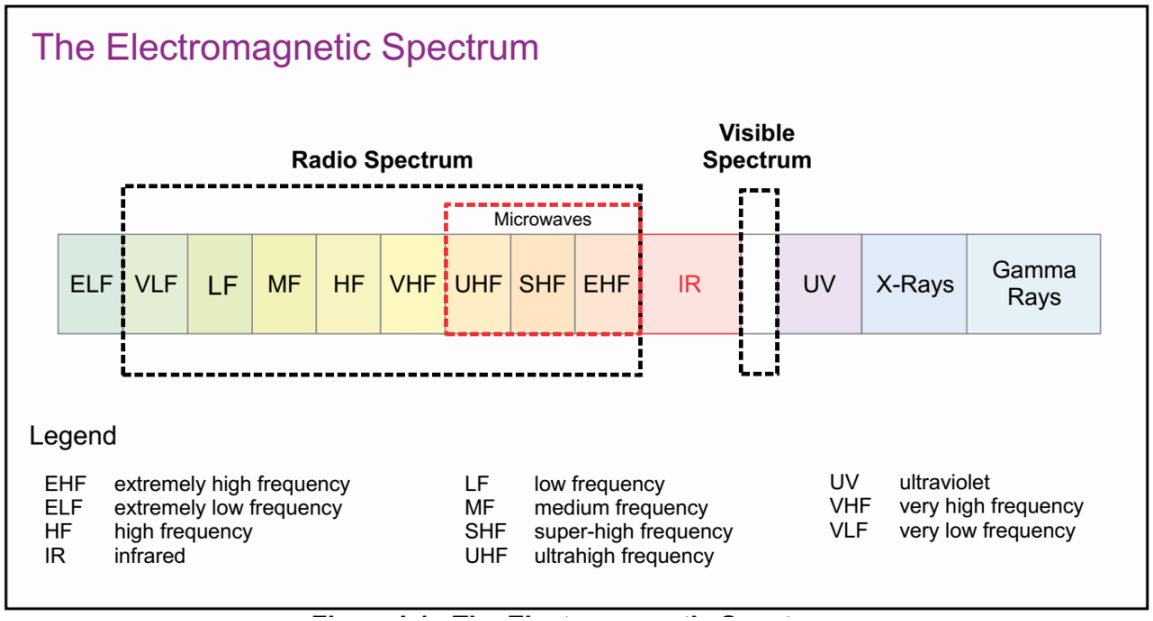

Figure 1.2. Electromagnetic spectrum overview. Source: [2]

Simultaneously, the complexity of this electronic battlefield is further illustrated in Fig. 1.3 [3], emphasizing the multifaceted nature of EW operations. As new sensors and radar systems push the boundaries of detection and precision, adversaries employ sophisticated tactics within the electromagnetic spectrum to disrupt and deceive. The interplay between technological advancements and adversarial EW strategies underscores the critical need for cutting-edge solutions, such as advanced signal processing techniques to maintain a robust defense against evolving threats.

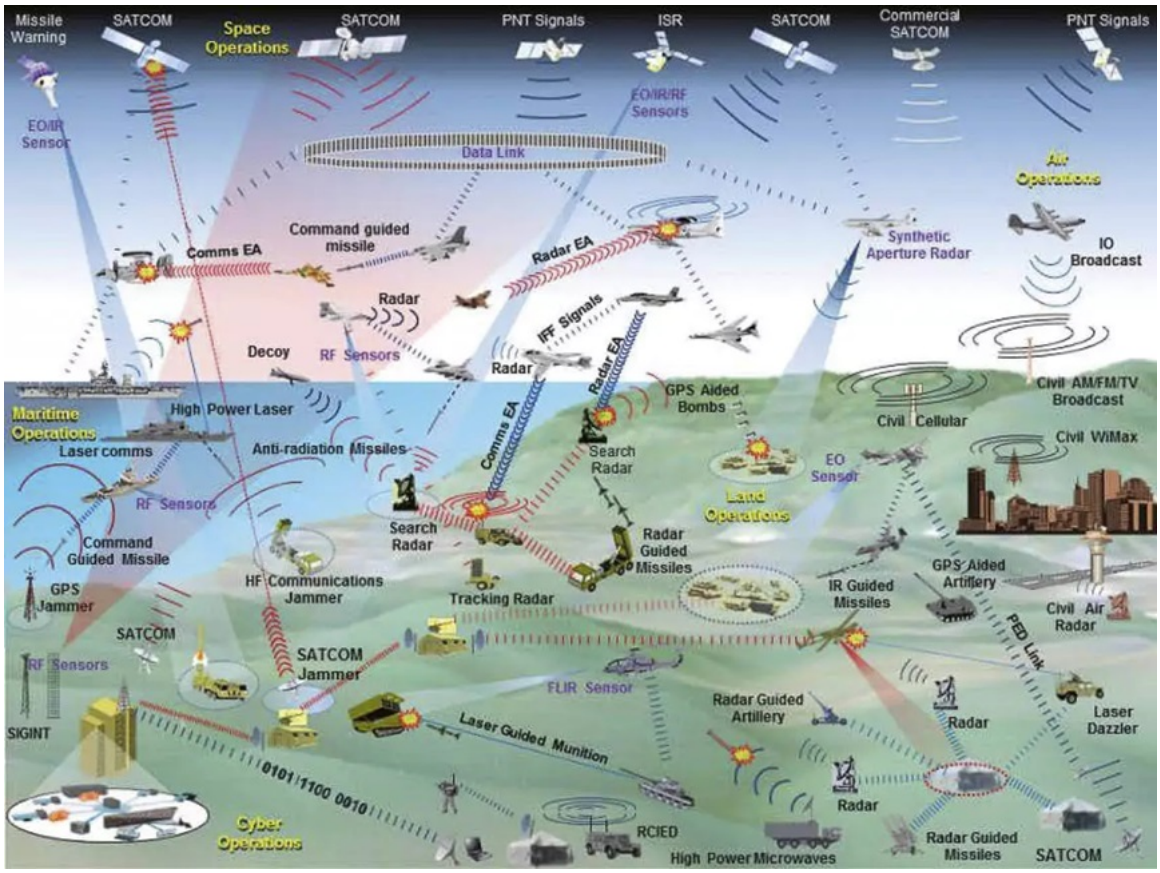

Figure 1.3. EW in Modern Warfare. Source: [3]

Within this EW landscape, strategies are traditionally categorized into three pillars: electronic attack (EA), electronic support (ES), and electronic protection (EP) [4]. EA involves deliberate interference to disrupt adversary systems, ES focuses on gathering intelligence through signal interception, and EP employs countermeasures to safeguard friendly systems against attacks.

As adversaries employ increasingly sophisticated EW tactics, it is imperative to comprehend how such interferences impact the performance of the radar systems.

Against this introductory backdrop, the subsequent section will delve deeper into the motivations driving this research, exploring the specific reasons behind the evaluation of degradation effects on detection performance caused by different types of interference on STAP radar.

1.1 Motivation

This research is driven by the need to evaluate the impact of advanced noise interference on a STAP receiver, specifically comparing it against conventional broadband noise interference, which is characterized by having a flat power spectral density within the operating frequency range of interest. Our focus extends beyond the theoretical understanding of interference types to practical solutions involving detection performance. By closely examining the vulnerabilities introduced by these advanced noise interferences, we aim to establish insights to enhance detection resilience within the evolving EW landscape.

1.2 Prior Research and Key Results

1.2.1 STAP

In conventional non-moving radars, spatial processing plays a central role in target detection and clutter suppression by distinguishing between echoes from stationary objects and moving targets. However, the challenge arises in moving airborne MTI radar systems, where traditional one-dimensional spatial processing is insufficient due to Doppler shifts caused by the motion of the radar platform. This leads to difficulties in distinguishing between ground clutter and potential target signals accurately.

Key Features of STAP

STAP is a well-established signal processing technique and is an excellent choice in enhancing target detection probability, particularly in environments where clutter undergoes Doppler shifts due to the motion of the radar platform [5]. STAP utilizes both temporal and spatial information and integrates them together to provide an effective solution for detecting targets amidst sea clutter. It is particularly effective in scenarios where conventional spatial processing proves insufficient.

Prior Research on STAP

In other research, STAP has been proven to effectively suppress dense false target interference with bi-phase random coded waveform by selecting the appropriate adaptive matched filter, thereby achieving a signal-to-interference plus noise-ratio (SINR) gain of above 20 dB [6]. STAP technique is also applied successfully to suppress sea clutter and strong interference signals to detect slow moving targets effectively using sample matrix inversion method and dimension-reduced $\sum \Delta$-STAP, which utilize both sum- and delta-channels to nullify clutter and interference achieving close to optimal processing [7].

1.2.2 EA

EA, a key focus of this research, employs both coherent and noncoherent interference to degrade the adversary radar detection capabilities. In most studies, as in [5], [6] and [8], noise interference is commonly assumed to be conventional additive white Gaussian noise (AWGN) and STAP has proven to be highly capable to spatially suppress and null these interferences and clutter when leveraging on techniques such as bi-phase random coding waveform and match filtering.

Coherent Interference

Coherent interference which is implemented by a digital RF memory (DRFM) device, involves manipulating the phase relationship between interference and radar signals. This strategic approach complicates the task of distinguishing genuine target echoes from noise, with advanced techniques like partially coherent noise interference, effectively degrading radar detection while conserving jamming power [9].

Non-coherent Interference

In contrast, non-coherent interference techniques, such as broadband noise interference, aim to decrease the receiver signal-to-noise ratio (SNR) by transmitting a high-energy level of noise. This intentional degradation of radar sensitivity increases the false alarm probability, presenting additional challenges in maintaining effective detection capabilities.

Transmit waveform shaped noise interference or jammer (TWS-NJ)
Beyond AWGN, an advanced type of interference is the transmit waveform shaped noise interference or jammer (TWS-NJ) [10]. The TWS-NJ is a highly effective noise interference designed to exploit specific vulnerabilities in the radar signal by intentionally mimicking the frequency characteristics of the radar transmitted waveform, creating confusion and increasing the difficulty of detecting target signals from interference.

It is important to note that TWS-NJ is not the same as a coherent interference [10]. While both coherent interference and TWS-NJ are employed in EA, they differ in their approach to interference, the timing of their transmissions and the complexity of their designs. Coherent interference typically responds to the radar transmission and becomes active when it detects the radar signal and attempts to interfere with the radar signal processing during the reception of the echoes.

Note that TWS-NJ may be implemented in a partially coherent manner by timing its transmission in relation to a target return. However, it does not necessarily wait for radar transmission but instead, it can proactively send noise vectors to disrupt the radar reception by creating false targets and flooding the radar receiver with noise. In general, designing and implementing a coherent interference can be more complex and require a good understanding of the radar signal characteristics, potentially making coherent interference systems more sophisticated and costlier. TWS-NJ design is less dependent on precise timing with radar transmission, allowing more flexibility in its implementation.

1.2.3 EP

To mitigate such advanced interference, modern radars are equipped with ES systems that use knowledge-based techniques about the electromagnetic spectrum to effectively avoid or filter out such interference [11]. These systems deploy EP methods or electronic counter-countermeasures (ECCM) techniques to preserve detection capability.

Research efforts are continuously invested to improve and ensure that the EP implementation is able to keep up with the advancement of EA. As mentioned in previous paragraphs, while the $\sum\Delta$-STAP can suppress sea clutter, it encounters performance limitations when the antenna scanning angle is larger than 4° [7].

Generalized Matched Filter

Another example of EP is the use of the generalized matched filter (GMF). The GMF is an adaptive filtering method used in radar signal processing and is designed to optimize the detection of signals in the presence of noise and interference when an accurate estimate of the interference covariance matrix is available by adjusting its filter characteristics adaptively [12].

The GMF is known for its adaptability to different signal environments. It adjusts its filtering characteristics based on the specific statistical properties of the received signals, hence making it well-suited for scenarios where the signal characteristics may vary. In addition, it exploits the knowledge about the statistical properties of the interference signal, enabling the filter to suppress the unwanted components effectively and focus on the desired signals to maximize the SINR.

In this research, we evaluated the performance of the GMF in the presence of various types of interference and how the GMF can be used to mitigate the impact of these interference and contribute to robust radar performance.

1.3 Research Question

In this research, we seek to analyze the impact of TWS-NJ on a STAP receiver and compare it to the conventional broadband noise interference or jammer (BB-NJ). Given the recent introduction of the TWS-NJ [10], the impact on detection performance and its effects on STAP is largely unexplored. The study aims to bridge this gap by building an understanding of its effects on signal detection performance within the cluttered environment.

Furthermore, we study the efficacy of the GMF as an EP measure against the TWS-NJ and analyze its effectiveness across various interference scenarios. These investigations are vital to establish a deeper understanding of radar signal processing and EW strategies in modern warfare.

1.4 Thesis Outline

This thesis consists of five chapters. In chapter 2, we establish the foundational understanding of STAP, clutter formation and detection theory. In chapter 3, we discuss the formulation of TWS-NJ and the EA and EP approaches on STAP. In chapter 4, we perform an empirical analysis to examine the effects of TWS-NJ on detection performance and evaluate the EP measures against it. The final chapter, chapter 5, consolidates key findings and identify areas for future exploration.

CHAPTER 2:
Background

In this chapter, we review and discuss key concepts to gain necessary background knowledge to contextualize the research conducted in this thesis. The primary focus on this chapter is to establish a foundational understanding of clutter and interference formation as well as detection theory, all of which are integral to understanding STAP radar systems.

2.1 Clutter Formation

Consider a side-looking airborne radar moving in the x-direction illustrated in Fig. 2.1. The radar is equipped with equally-spaced N antenna elements aligned with the direction of motion. Each antenna is separated by a distance $d = \frac{\lambda}{2}$, where λ is the operating wavelength corresponding to the carrier frequency. The radar, traveling at velocity v, transmits a series of M coherent pulses and the resulting echo returns are collected by the antennas. Note that the radar beam width is primarily determined by the number of antenna elements and is not inherently linked to the dimensions of the clutter patches.

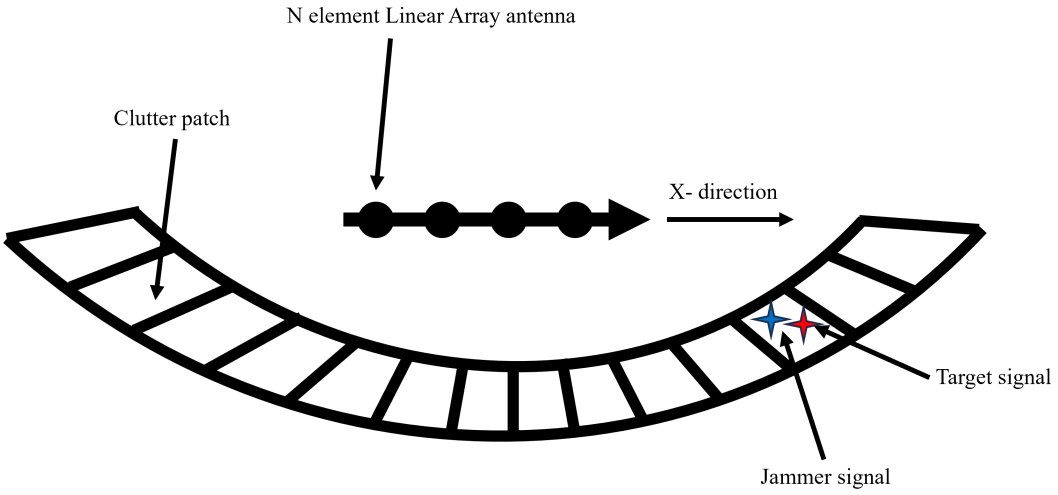

Figure 2.1. Illustration of MTI Radar.

To better understand clutter formation, we focus on practical scenarios where small depression angles θ, and curved Earth effects can be safely ignored while the radar platform is in motion. This simplification allows us to gain an understanding on the concept of clutter ridges, which emerge due to Doppler shifts induced by the radar platform's motion or the movement of objects within the radar beam. The ground clutter energy is distributed along a line, which forms what is commonly known as the clutter ridge [5] as shown in Fig. 2.2. This spatial variation in clutter introduces a challenge, particularly when the target and interference signals align within the same clutter angle. This alignment significantly impedes the radar receiver's ability to detect the desired signal while simultaneously suppressing the interference signal.

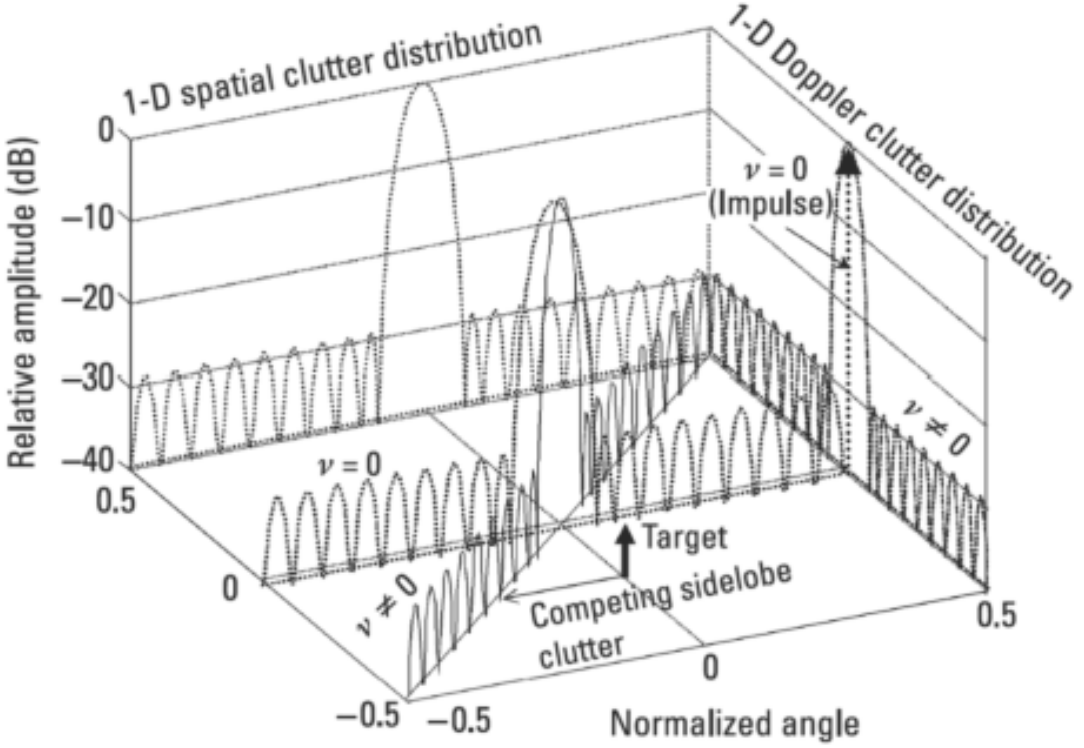

Figure 2.2. Illustration of Clutter Ridge. Source: [5]

2.2 Clutter Covariance Matrix Derivation

The clutter covariance matrix is a crucial component as it captures the statistical properties of clutter returns in the radar system. It is computed as the expected value of the outer product of the clutter steering vector $\mathbf{v}_c$. This matrix helps us understand how clutter signals are distributed across different spatial and temporal dimensions, providing a crucial foundation for clutter suppression techniques.

As illustrated in Fig. 1.1, to quantify the total clutter return given an iso-range, the clutter covariance matrix $\mathbf{R}_c$ is given by:

$$\mathbf{R}_c = \mathbb{E}\{\mathbf{v}_c \mathbf{v}_c^H\}, \tag{2.1}$$

where $\mathbf{v}_c$ represents the clutter steering vector, $\mathbb{E}$ is the expected value operator, and H is the Hermitian operator [5]. The signal vector in each clutter angle is represented by the Kronecker product of the Doppler and spatial steering vectors $\mathbf{b}_i$ and $\mathbf{a}_i$ respectively, By letting M be the number of pulses and N be the number of antenna elements, $\mathbf{v}_i$ is the $NM\times 1$ space-time steering vector for the ith spatial-Doppler cell. Thus,

$$\mathbf{v}_i = \mathbf{b}_i \otimes \mathbf{a}_i, \tag{2.2}$$

where $\mathbf{b}_i$ and $\mathbf{a}_i$ are of the form

$$\mathbf{a}_i = \begin{bmatrix} 1 & e^{j2\pi\overline{f}_s} \cdots e^{j2\pi(N-1)\overline{f}_s} \end{bmatrix}^T, \tag{2.3}$$

$$\mathbf{b}_i = \begin{bmatrix} 1 & e^{j2\pi\overline{f}_d} \cdots e^{j2\pi(M-1)\overline{f}_d} \end{bmatrix}^T, \tag{2.4}$$

where T is the transpose operator, $\overline{f}_s$ and $\overline{f}_d$ denote the normalized spatial and Doppler frequencies respectively [5].

2.3 Interference Covariance Matrix Derivation

The interference covariance matrix characterizes the interference noise in the radar system and plays a vital role towards understanding and then mitigating the impact of interference on radar performance.

In the derivation of the interference covariance matrix, a common assumption is a single sample per pulse, where the interference is considered to be uncorrelated from pulse-to-pulse. Hence, the off-diagonal sub-covariance blocks are null matrices. In other words, the $NM \times NM$ single pulse interference covariance matrix R_j exhibits the following block diagonal form:

$$\mathbf{R}_j = \begin{bmatrix} \sigma_j^2 \mathbf{s}_j \mathbf{s'}_j & & & \oslash \\ & \sigma_j^2 \mathbf{s}_j \mathbf{s'}_j & & \vdots \\ \vdots & & \ddots & \\ \oslash & & & \sigma_j^2 \mathbf{s}_j \mathbf{s'}_j \end{bmatrix}, \tag{2.5}$$

where σ_j^2 is the interference noise variance. The vector $\mathbf{s}_j$ serves as the interference steering vector associated with a plane wave angle of arrival, representing the direction from which the interference signal impinges upon an antenna array with N equally spaced elements [5]. This vector consists of complex weights assigned to each antenna element, shaping the spatial characteristics of the interference signal across the array.

2.4 Conventional STAP Covariance Matrix Derivation

The STAP covariance matrix $\mathbf{R}$ combines information from clutter, interference and thermal noise sources. The matrix is fundamental in the development of STAP algorithms, enabling a radar system to differentiate between desired signals and unwanted noise components. In the derivation of the conventional STAP covariance matrix, we begin by assuming the receiver noise to be AWGN and statistically independent of the clutter and interference noise. Assuming zero-mean interference processes and letting $\mathbf{R}_c$ and $\mathbf{R}_j$ be the clutter and interference covariance matrices respectively, the conventional overall STAP covariance matrix, $\mathbf{R}$, therefore has the form

$$\mathbf{R} = \mathbf{R}_c + \mathbf{R}_j + \sigma^2 \mathbf{I}_{NM}, \tag{2.6}$$

where σ^2 is the thermal noise sample variance and $\mathbf{I}_{NM}$ is the $NM \times NM$ identity matrix. The dimension of the conventional STAP covariance matrix is therefore $NM \times NM$. It is crucial to recall that the conventional STAP receiver formulation assumes only one sample of received signal (consisting of the target signal, clutter, thermal and interference noises) per pulse.

2.5 Detection Theory

A quick detection theory review is in order to understand conventional STAP detection and to set the stage subsequently to understand both EA effects and EP mitigation of TWS-NJ on STAP in latter chapters. In conventional STAP, there are two hypotheses, H_0 and H_1 [12], which are defined as:

$$\begin{aligned} H_0 &: \tilde{\mathbf{x}}[n] = \tilde{\mathbf{w}}_n, \\ H_1 &: \tilde{\mathbf{x}}[n] = \tilde{\mathbf{s}}_n + \tilde{\mathbf{w}}_n, \end{aligned} \tag{2.7}$$

where $\tilde{\mathbf{x}}$ is the received complex signal vector. The hypothesis H_1 denotes the presence of the known target signal vector $\tilde{\mathbf{s}}_n$, and $\tilde{\mathbf{w}}_n$ is the colored noise vector consisting of clutter, interference and thermal noise. The null hypothesis H_0 denotes presence of $\tilde{\mathbf{w}}_n$ only. The likelihood ratio test to decide H_1 is given by:

$$L_{(\tilde{x})} = \frac{p(\tilde{\mathbf{x}}; H_1)}{p(\tilde{\mathbf{x}}; H_0)} > \gamma_L, \tag{2.8}$$

where γ_L is the likelihood ratio threshold. The probability density functions for detection are:

$$\begin{aligned} p(\tilde{\mathbf{x}}; H_1) &= \frac{1}{\pi^N \det(\mathbf{R})} \exp\left[-(\tilde{\mathbf{x}} - \tilde{\mathbf{s}})^H \mathbf{R}^{-1} (\tilde{\mathbf{x}} - \tilde{\mathbf{s}})\right], \\ p(\tilde{\mathbf{x}}; H_0) &= \frac{1}{\pi^N \det(\mathbf{R})} \exp\left[-\tilde{\mathbf{x}}^H \mathbf{R}^{-1} \tilde{\mathbf{x}}\right], \end{aligned} \tag{2.9}$$

where $\tilde{\mathbf{s}}$ is the known target steering vector, “det" is the determinant operator and $\mathbf{R}$ refers to the conventional STAP covariance matrix with $NM \times NM$ dimension as previously outlined in (2.6).

THIS PAGE INTENTIONALLY LEFT BLANK

CHAPTER 3:
Implementation

This chapter is dedicated to introducing the TWS-NJ signal and examining its impact on STAP detection. In contrast to common literature assumptions [5], [6] and [8] that often consider interference signals to be AWGN, TWS-NJ, as a shaped interference, is inherently correlated (colored). Additionally, it is common for the interference noise to be considered as single sample per pulse, thus making the standard formulation in (2.6) inadequate in capturing TWS-NJ characteristics which should have multiple samples per pulse in order to capture the correlated nature of this interference. The chapter will also discuss EP implementation using GMF as a mitigation technique to the noise interference and highlight the significance of having an accurate estimation of the interference covariance matrix to augment the overall STAP covariance matrix for enhanced detection capabilities.

3.1 TWS-NJ Covariance Matrix

As previously discussed, the TWS-NJ differs significantly from broadband noise interference as it leverages on the spectral characteristics of the radar waveform to construct the interference. Notably, the noise samples within each pulse exhibit correlation. This renders the one-sample-per-pulse signal model, which is common in typical STAP formulations to be insufficient for accurate signal modeling in the case of TWS-NJ. To effectively represent TWS-NJ interference and enable STAP EP implementation, multiple samples per pulse are necessary for pulse shaping, enabling the formation of a larger covariance matrix.

Consider the parameter K, representing the number of samples in a single pulse. If we let $\mathbf{s}$ to be a unit-energy transmit waveform, then a convolution matrix $\mathbf{H}_s$ is formed. From the convolution matrix, the resulting auto-correlation matrix is then expressed as:

$$\mathbf{R}_h = \mathbf{H}_s^H \mathbf{H}_s, \tag{3.1}$$

where $\mathbf{R}_h$ is clearly a $K \times K$ matrix. This covariance matrix helps shape the interference noise realization using the transmit waveform characteristics.

Recall that in a typical one-sample per pulse STAP formulation, the covariance matrix for the interference in (2.5) has a matrix rank of one. In the case of (3.1), $\mathbf{R}_h$ can be of rank K. However, just like in conventional STAP, it is still reasonable to assume that the interference noise is independent from one pulse to the next despite the correlation within a single pulse. Let $\mathbf{R}_{jj}$ denote the correlation matrix derived by using only the spatial steering vector via (2.3) for a given noise interference. By taking the Kronecker product of $\mathbf{R}_h$ with each entry of $\mathbf{R}_{jj}$, then an expanded single pulse TWS-NJ covariance matrix $\mathbf{R}_{js}$ corresponding to K samples and N antenna elements is formed by:

$$\mathbf{R}_{js} = \begin{bmatrix} \mathbf{R}_{jj}(1,1)\left[\mathbf{R}_h\right] & \cdots & \mathbf{R}_{jj}(1,N)\left[\mathbf{R}_h\right] \\ & & \vdots \\ \vdots & \ddots & \\ \mathbf{R}_{jj}(N,1)\left[\mathbf{R}_h\right] & \cdots & \mathbf{R}_{jj}(N,N)\left[\mathbf{R}_h\right] \end{bmatrix}, \tag{3.2}$$

where $\mathbf{R}_{js}$ is the single-pulse TWS-NJ covariance matrix with $NK \times NK$ dimension from a particular angular direction.

As an example of illustrating the correlated multiple samples in a single Hamming-shaped pulse, the 2-D image (intensity) map of TWS-NJ covariance matrix as discussed in (3.2) is illustrated in Fig. 3.1 and its 3-D (magnitude) map is illustrated in Fig. 3.2.

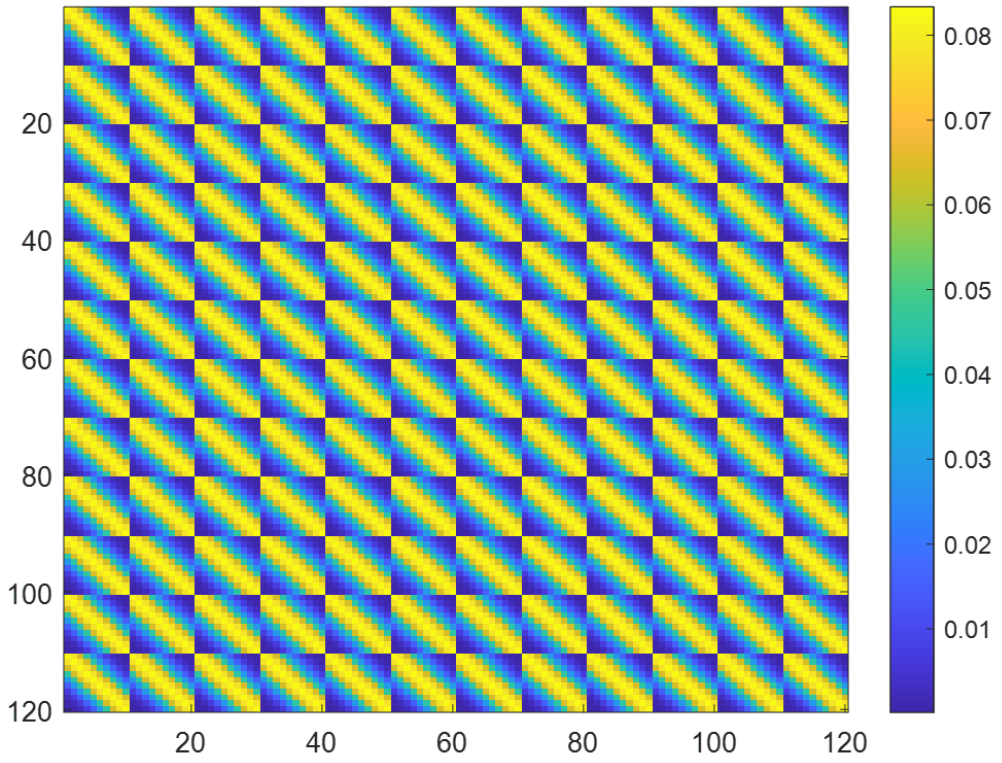

Figure 3.1. 2-D image (intensity) map of a Hamming-shaped TWS-NJ covariance matrix.

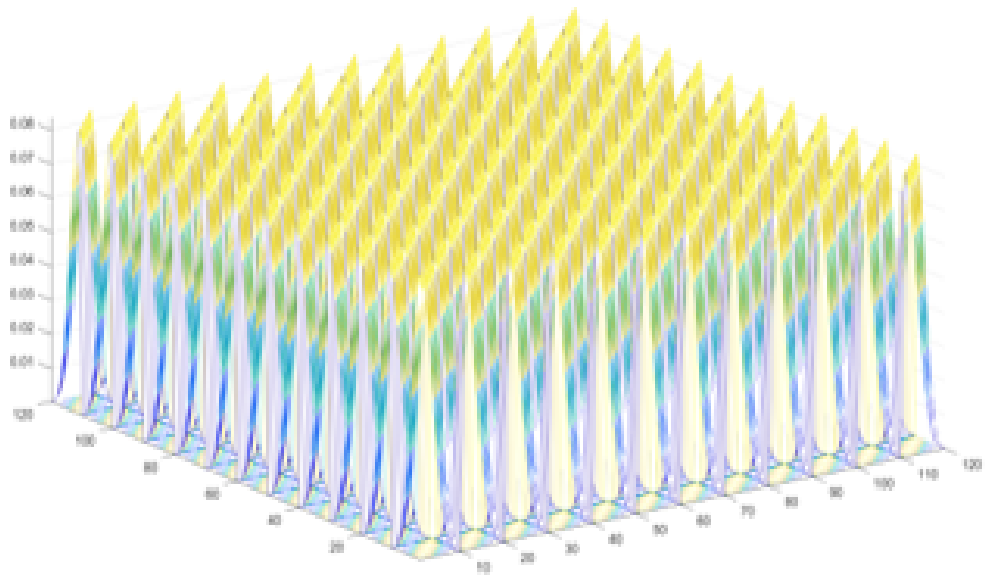

Figure 3.2. 3-D (magnitude) map of a Hamming-shaped TWS-NJ covariance matrix.

The final step in incorporating multiple pulses M into the TWS-NJ covariance matrix is achieved by performing another Kronecker product of $\mathbf{R}_{js}$, shown in (3.2), with an identity matrix of dimension M. This operation results in the formation of M multiple-pulse TWS-NJ covariance matrix, denoted as $\mathbf{R}_{tws}$ given by:

$$\mathbf{R}_{tws} = \begin{bmatrix} \left[\mathbf{R}_{js}\right] & & & \oslash \\ & \left[\mathbf{R}_{js}\right] & & \vdots \\ \vdots & & \ddots & \\ \oslash & & & \left[\mathbf{R}_{js}\right] \end{bmatrix} \tag{3.3}$$

Here, $\mathbf{R}_{tws}$ is the multiple-pulse TWS-NJ covariance matrix with the dimension of $NMK \times NMK$. It is noteworthy that in contrast to the conventional STAP covariance matrix described in (2.6), which has the dimension of $NM \times NM$, the final STAP covariance matrix is clearly larger ($NMK \times NMK$).

This size increase is due to the incorporation of pulse shaping which is inherent in TWS-NJ. The covariance matrix $\mathbf{R}_{tws}$ captures the spatial and temporal characteristics of the interference. For accurate EP implementation, a precise estimate of this covariance matrix is essential and details on the use of this covariance matrix for detection will be covered in the subsequent section.

3.2 Implementing the EA Effects of TWS-NJ on STAP

Pulse-shaping of the TWS-NJ significantly impacts the overall STAP covariance matrix. With the increased in dimension by K samples, the contribution of the TWS-NJ covariance matrix $\mathbf{R}_{tws}$ becomes pivotal. The overall STAP covariance matrix from (2.6) is augmented into the following form:

$$\mathbf{R}_{stap} = \mathbf{R}_{c,tws} + \mathbf{R}_{tws} + \sigma^2 \mathbf{I}_{NMK}, \tag{3.4}$$

where $\mathbf{R}_{stap}$ and $\mathbf{R}_{c,tws}$ are the enlarged overall STAP covariance matrix and clutter covariance matrix respectively with the dimension of $NMK \times NMK$ as compared to (2.6). Therefore, this highlights the specific impact of TWS-NJ pulse-shaping on the covariance matrix dimensions and the importance of $\mathbf{R}_{tws}$ in STAP.

In this implementation, two shaped interference – Hamming and rectangular pulse – are generated, and their impact is compared against the BB-NJ. Various scenarios, including different TWS-NJ placements relative to the target signal within clutter, are examined to assess STAP detection performance comprehensively.

3.3 EP Implementation Using GMF

In response to the EA effect induced by TWS-NJ, we proceed with the EP implementation using the GMF. The GMF is a natural choice in EP implementation given its versatile performance as an optimum detector in correlated noise such as that induced from the TWS-NJ. As in any adaptive matched filter approach, an ES receiver support is assumed and hence, an accurate temporal covariance matrix corresponding to the TWS-NJ is available to be incorporated into the overall STAP covariance matrix described in (3.4).

Using (2.9), H_1 can be determined if

$$T(\tilde{\mathbf{x}}_{stap}) = \mathrm{Re}(\tilde{\mathbf{s}}_{stap}^H \mathbf{R}_{stap}^{-1} \tilde{\mathbf{x}}_{stap}) > \gamma, \tag{3.5}$$

where γ represents the detection threshold that defines the decision boundary between the presence or absence of a target. Note that $\tilde{\mathbf{x}}_{stap}$, $\tilde{\mathbf{s}}_{stap}$ are also augmented to represent the enlarged dimension of $NMK\times1$ as compared to its $NM\times1$ versions in (2.7). $\mathbf{R}_{stap}^{-1}$ is the inverse of the overall STAP covariance matrix. $\mathbf{R}_{stap}^{-1}$ is crucial to compute the adaptive weights for both antenna elements and temporal taps to enhance the contribution of signals of interest while simultaneously suppressing clutter and the TWS-NJ. As illustrated in Fig. 3.3, we first note that $\tilde{z}_{stap} = \tilde{\mathbf{x}}_{stap}^H \mathbf{R}_{stap}^{-1} \tilde{\mathbf{x}}_{stap}$ is a complex Gaussian random variable since it is a linear transformation of the complex Gaussian random vector $\tilde{\mathbf{x}}_{stap}$ [12]. Then it can be shown that

$$\begin{aligned}
&\mathbb{E}(\tilde{z}_{stap}; H_0) = 0 \\
&\mathbb{E}(\tilde{z}_{stap}; H_1) = \tilde{\mathbf{x}}_{stap}^H \mathbf{R}_{stap}^{-1} \tilde{\mathbf{x}}_{stap} \\
&\mathrm{var}(\tilde{z}_{stap}; H_0) = \mathrm{var}(\tilde{z}_{stap}; H_1) = \tilde{\mathbf{x}}_{stap}^H \mathbf{R}_{stap}^{-1} \tilde{\mathbf{x}}_{stap},
\end{aligned} \tag{3.6}$$

therefore $T(\tilde{\mathbf{x}}_{stap})$ can be expressed as

$$T(\tilde{\mathbf{x}}_{stap}) \sim \begin{cases} \mathcal{N}(0, \tilde{\mathbf{x}}_{stap}^H \mathbf{R}_{stap}^{-1} \tilde{\mathbf{x}}_{stap}/2) & \text{under } H_0, \\ \mathcal{N}(\tilde{\mathbf{x}}_{stap}^H \mathbf{R}_{stap}^{-1} \tilde{\mathbf{x}}_{stap}, \tilde{\mathbf{x}}_{stap}^H \mathbf{R}_{stap}^{-1} \tilde{\mathbf{x}}_{stap}/2) & \text{under } H_1, \end{cases} \tag{3.7}$$

where $\mathcal{N}$ denotes a normal (Gaussian) distribution. Under the null hypothesis H_0, the test statistic $T(\tilde{\mathbf{x}}_{stap})$ follows a normal distribution with a mean of 0 and variance of $\tilde{\mathbf{x}}_{stap}^H \mathbf{R}_{stap}^{-1} \tilde{\mathbf{x}}_{stap}/2$. Conversely under the alternative hypothesis H_1, the mean shifts to $\tilde{\mathbf{x}}_{stap}^H \mathbf{R}_{stap}^{-1} \tilde{\mathbf{x}}_{stap}$ while the variance remains $\tilde{\mathbf{x}}_{stap}^H \mathbf{R}_{stap}^{-1} \tilde{\mathbf{x}}_{stap}/2$.

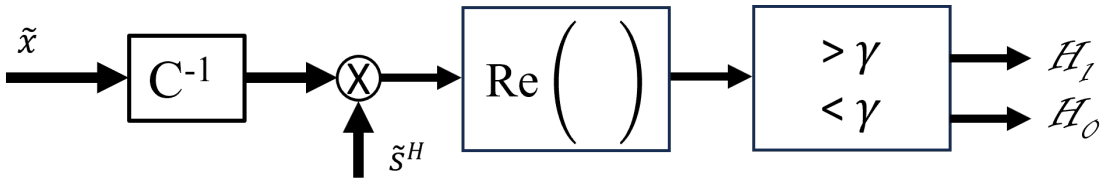

Figure 3.3. GMF for complex data. Source [12]

Therefore, the detection threshold γ is given by:

$$\gamma = \sqrt{\tilde{\mathbf{s}}_{stap}^H \mathbf{R}_{stap}^{-1} \tilde{\mathbf{s}}_{stap}/2} Q^{-1}(P_{FA}), \tag{3.8}$$

which is well-established in [12] and P_{FA} is the probability of false alarm. The probability of detection performance is thus:

$$P_D = Q(Q^{-1}(P_{FA}) - \sqrt{2 \times (\tilde{\mathbf{s}}_{stap}^H \mathbf{R}_{stap}^{-1} \tilde{\mathbf{s}}_{stap})}), \tag{3.9}$$

where $Q(\cdot)$ is the Q-function of the standard Gaussian distribution.

3.4 Monte Carlo Simulation

Monte Carlo (MC) simulation is a powerful computational technique in statistical modeling and random sampling to analyze the behavior of complex systems under uncertainty. In radar signal processing, MC simulation proves to comprehensively assess the performance and robustness of signal implementations such as the proposed TWS-NJ in STAP.

In MC simulation, multiple random samples, each representing a distinct set of system parameters are generated. In the context of this study, MC simulation facilitates the examination of diverse scenarios, encompassing variations in clutter conditions, TWS-NJ placements, and waveform characteristics. This detailed analysis provides a better understanding of how the integration of the proposed TWS-NJ in STAP along with the subsequent EP implementation, responds to fluctuations in the simulated environment.

THIS PAGE INTENTIONALLY LEFT BLANK

CHAPTER 4:
Performance Results and Analysis

This chapter presents the simulation results assessing the impact of TWS-NJ on STAP for target detection. Covariance matrices for TWS-NJ and BB-NJ are generated, with intensity maps illustrated in subsequent section. Analysis focuses on detection performance in clutter scenarios, with and without Electronic Protection (EP) implementation. The chapter also examines scenarios where the target and noise interference signals are spatially separated. The effectiveness of the Generalized Matched Filter (GMF) as a STAP EP technique is assessed, providing insights into its capability to counter challenges posed by TWS-NJ.

4.1 Simulation Setup

The system for our simulation contains a 12-element uniform linear array, transmitting a 16-pulse coherent processing interval (CPI) and receiving 10 samples within each pulse. For realistic conditions, we set clutter-to-noise ratio (CNR) at 40 dB following established examples [5] and we explore jammer-to-noise ratio (JNR) values ranging from 5–10 dB.

To generate the clutter covariance matrix, a clutter power spectral density (PSD) is used. In our simulation, the clutter environment is divided into 32 clutter patches given an iso-range to yield a well-represented clutter covariance matrix. The spatial or angular cells, corresponding to the number of antenna elements N, are indexed from 1–12.

To analyze the impact on detection performance, Monte Carlo simulations of 10,000 trials are conducted per received SNR value. The required P_{FA} is set at 10^{-4} and the thermal noise variance is set to unity for computational convenience.

We generate two TWS-NJs: one Hamming-shaped TWS-NJ and the other a rectangular-shaped TWS-NJ, using the methodology established in the preceding chapter. The TWS-NJs are then specifically matched with their corresponding target signals to simulate noise interference.

As a baseline for comparison against the TWS-NJ, we use BB-NJ which as previously mentioned, is the broadband noise interference characterized by having a flat power spectral density within the operating frequency range of interest. This investigation allows us to assess the performance of both the EA interference and the EP mitigation against it.

4.2 Results

Using (3.3), we create the 1920×1920 TWS-NJ and BB-NJ covariance matrices. As an example, the TWS-NJ (Hamming) and BB-NJ covariance matrix intensity maps are illustrated in Fig. 4.1 and Fig. 4.2. Of note, the BB-NJ covariance matrix would have been only 192×192 in conventional STAP where only one sample is used and the interference subcovariance would simply be rank one. For TWS-NJ, the subcovariance matrix for a single pulse is clearly full rank.

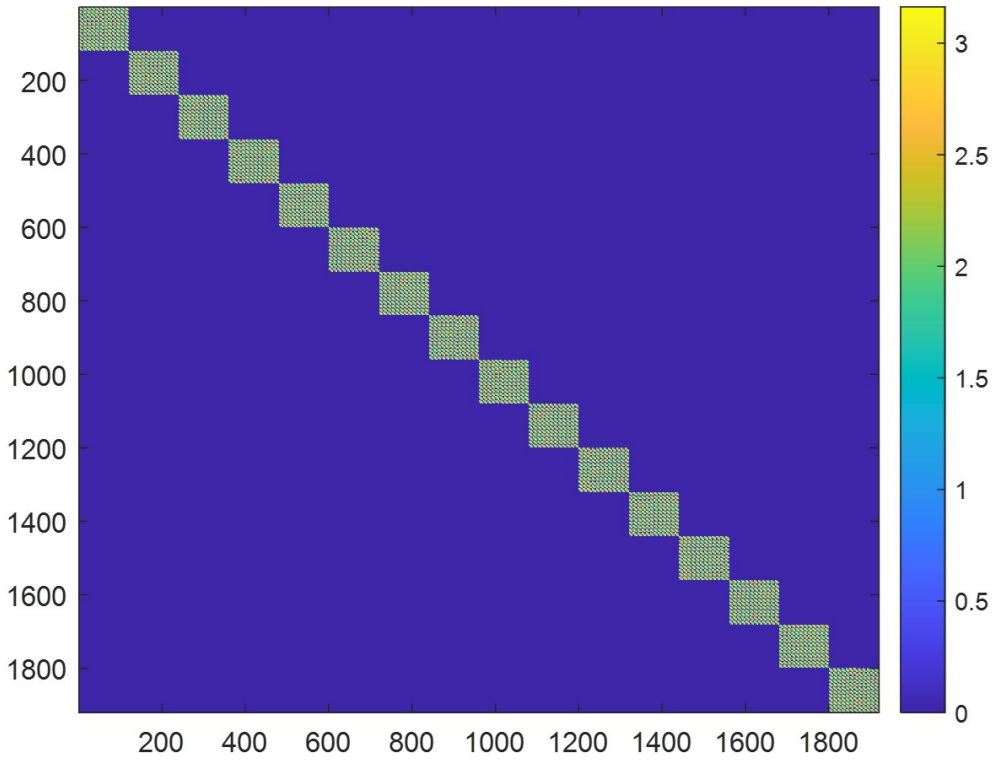

Figure 4.1. 2-D image (intensity) map of the TWS-NJ (Hamming) covariance matrix.

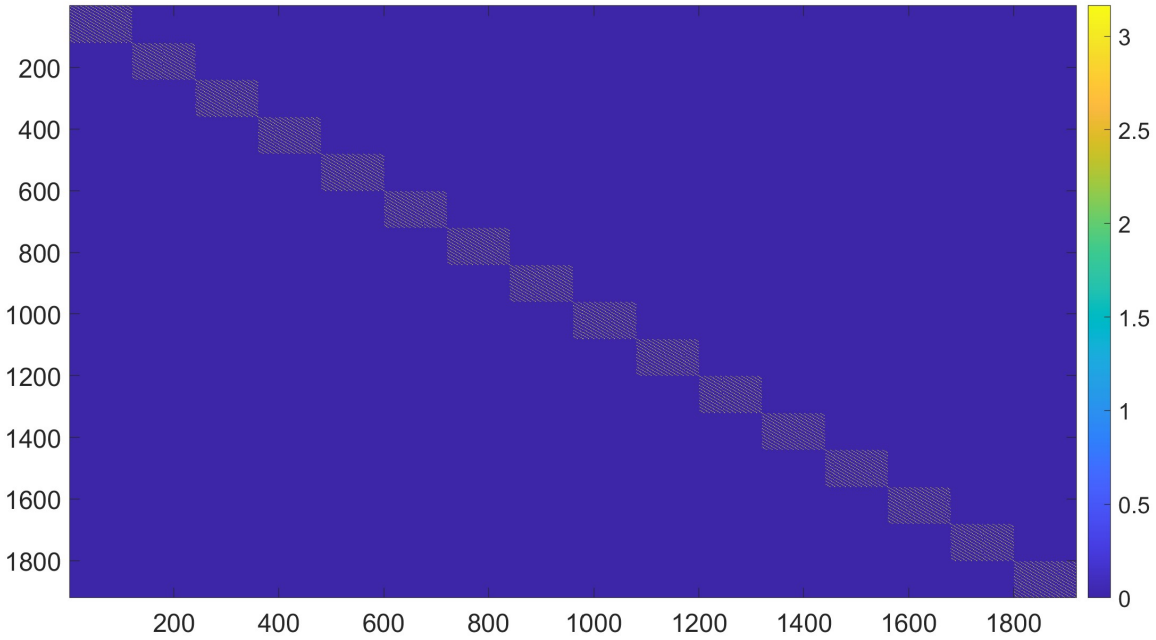

Figure 4.2. 2-D image (intensity) map of the BB-NJ covariance matrix.

The resulting P_D vs SNR detection performance curves depicted in subsequent figures reflect a few of the target and interference configurations.

4.2.1 Detection Performance for Target and Noise Interference Signals in the same Spatial Cell

Without EP Implementation

In this scenario, we evaluate the STAP receiver detection performance under EA without the implementation of EP. Notably, both the target and noise interference are placed in cell 9 of the spatial dimension. The target and noise interference are strategically placed together to realistically simulate a scenario whereby the target is equipped with self-protection jammer aimed to avoid detection by the MTI radar. The absence of EP allows for a focused examination of the noise interference capabilities of TWS-NJs and their effects on STAP detection performance.

A few observations are in order when the noise interference and the target are located in the same spatial or angular cell. First, for the radar under EA from the noise interference (i.e., without EP implementation yet), it is evident in the detection curves in Fig. 4.3 and Fig. 4.4 that the TWS-NJ proves to be a superior noise interference compared to the BB-NJ in terms of degrading P_D at high SNR.

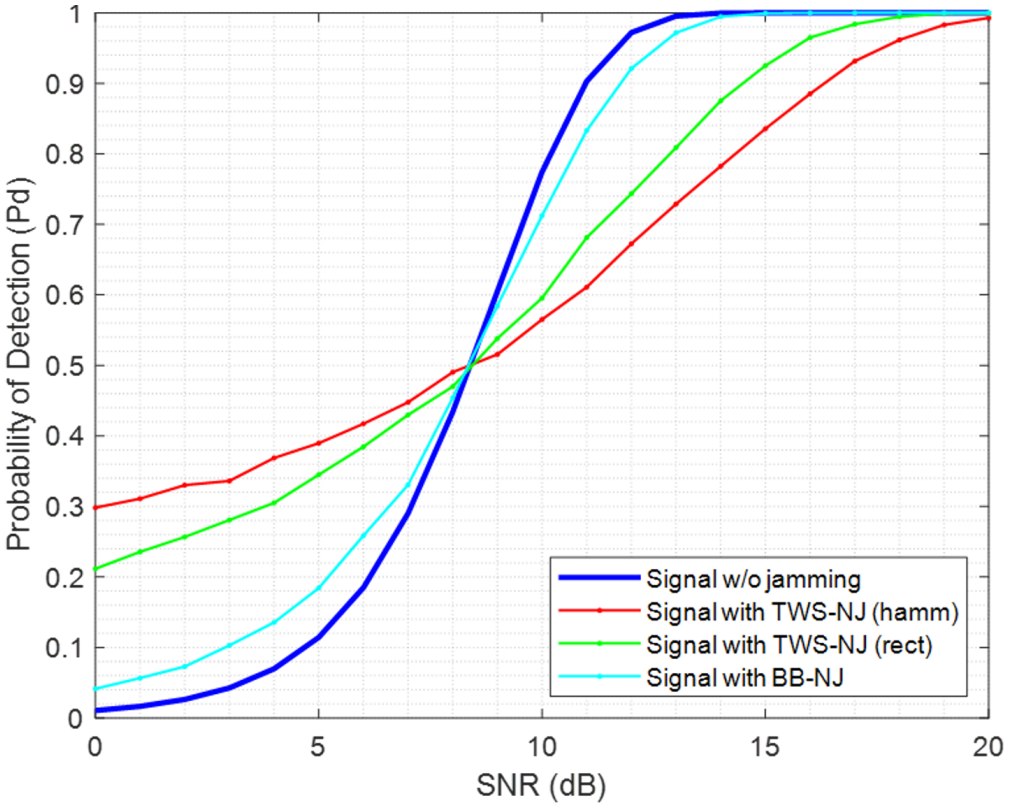

Figure 4.3. P_D vs SNR detection performance curves under EA w/o EP yet. JNR = 5 dB. Both target and noise interference signals are co-located in spatial cell 9.

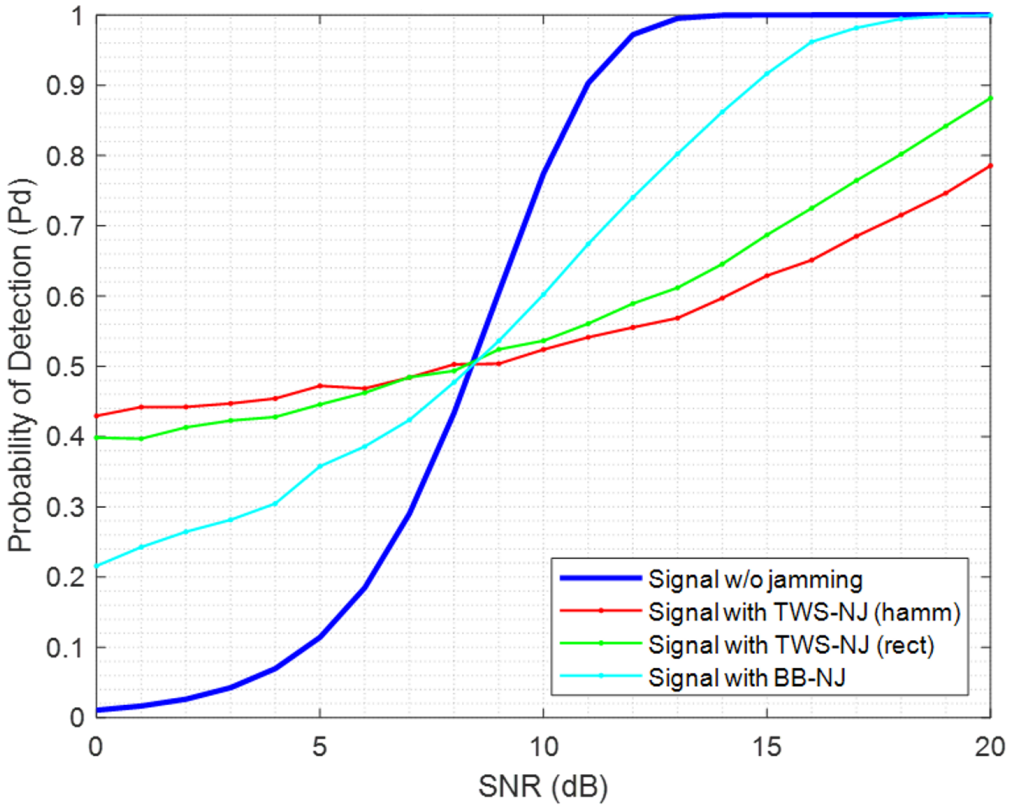

Figure 4.4. P_D vs SNR detection performance curves under EA w/o EP yet. JNR = 10 dB. Both target and noise interference signals are co-located in spatial cell 9.

The performance disparity between the TWS-NJs and the BB-NJ also widens as the JNR value increases from 5 dB in Fig. 4.3 to 10 dB in Fig. 4.4. This implies that the specific waveform shaping employed by the TWS-NJ, in conjunction with its strategic placement, resulted in a more pronounced interference thereby making target detection more challenging for the STAP algorithm. In addition, the design of the TWS-NJ features reduced sidelobes, enabling it to concentrate its energy into a more defined main beam to outperform the BB-NJ in terms of noise interference effectiveness. As comparison, the energy spectral density (ESD) of the two TWS-NJs are illustrated in Fig. 4.5 showing the reduced sidelobes.

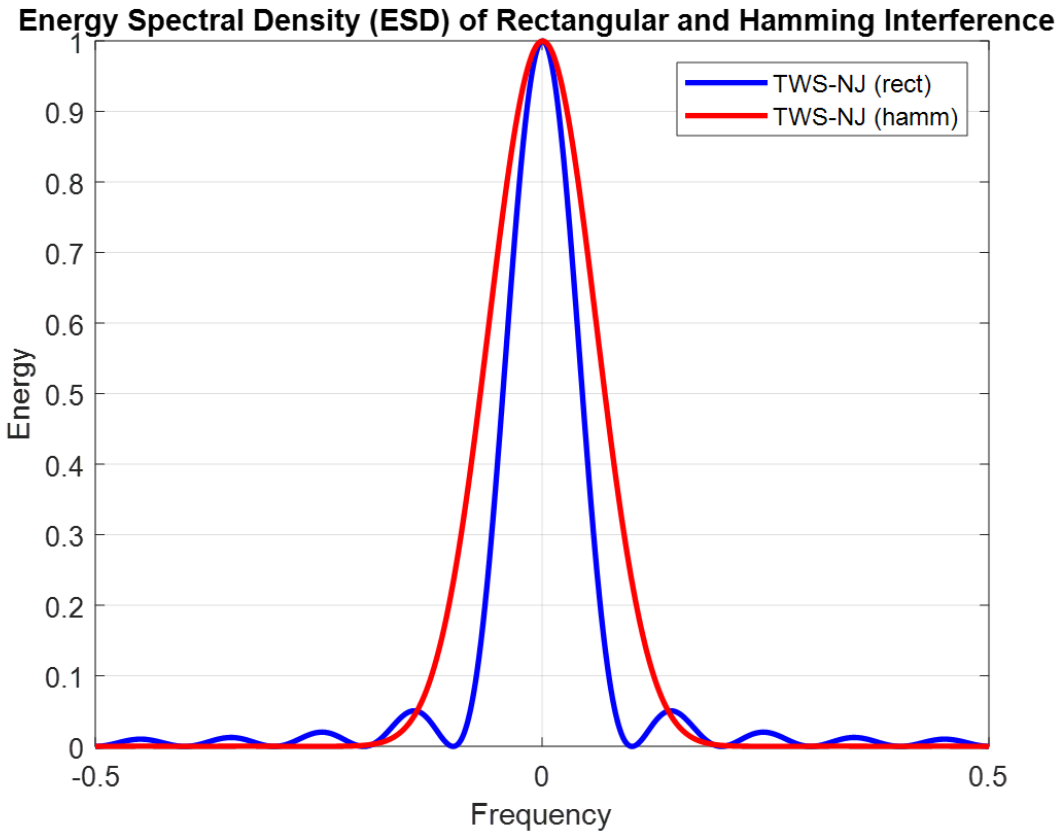

Figure 4.5. ESDs for TWS-NJ (rect) and (hamm).

Lastly, based on the observations in Fig. 4.3 and Fig. 4.4, it is evident that the Hamming transmit waveform and TWS-NJ (hamm) pair demonstrates superior noise performance over the rectangular transmit waveform and TWS-NJ (rect) pair. However, a different picture emerges upon further simulations involving different angular cells. In most cases, the TWS-NJ (rect) in fact, surpasses the TWS-NJ (hamm) when both the target and noise interference are positioned at other angles, as illustrated in Fig. 4.6 where the target and interference signal are co-located in spatial cell 8.

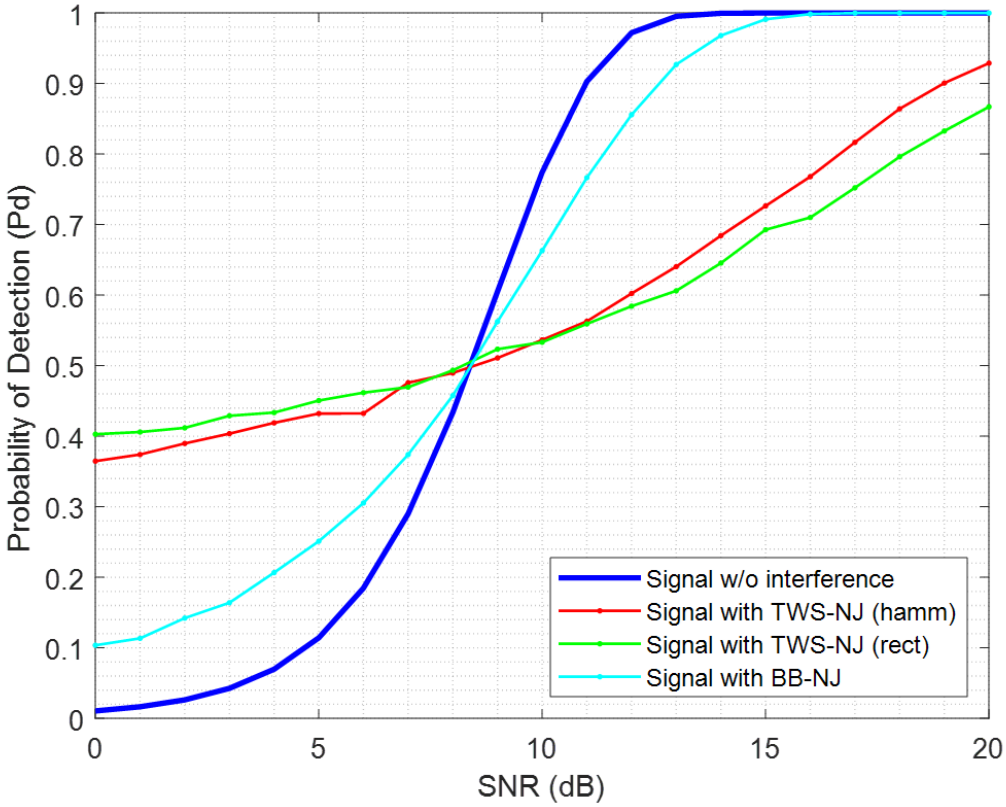

Figure 4.6. TWS-NJ (rect) outperforms TWS-NJ (hamm) when target and interference at other angles. Both target and interference signals are co-located in spatial cell 8.

This performance discrepancy underscores the significance of pulse shape in directing noise interference energy effectively. Recall in Fig. 4.5, the inherent characteristics of TWS-NJ (rect) contributes to a more precise concentration of energy in a narrower main beam (although the side lobes are higher), enhancing its ability to better disrupt target detection. Therefore, this further observed trend suggests that the choice of noise interference shape in TWS-NJs plays a pivotal role, with a more precise concentration of noise energy in the main beam leading to better interference effectiveness.

With EP Implementation

For the implementation of EP on the STAP receiver, we leverage on the GMF which is known for its robustness in handling correlated noise as discussed in the previous chapter. As we explore the results in the subsequent figures, it becomes apparent how the GMF excels in suppressing the noise interference while optimizing SINR.

From Fig. 4.7 to Fig. 4.9 where both the target signal and interference signals are co-located in spatial cell 9, it is evident that the detection performance remained closely aligned with the theoretically calculated values. This alignment proves the robustness of the EP strategy implemented using the GMF. The effectiveness of GMF becomes particularly pronounced considering that the noise interference is co-located with the target in the same spatial cell.

As mentioned, the success of the GMF to achieve optimal SINR while concurrently suppressing noise interference is realised through the incorporation of the estimated interference covariance matrix in the inverse STAP covariance matrix operation as described in (3.4). The inclusion of the interference covariance matrix empowers the GMF to precisely nullify the noise interference and preserve the detection performance of the STAP receiver.

In addition, the efficacy of the GMF to mitigate noise interference span across all JNR values investigated, underlining its versatility and applicability in diverse EA scenarios. The consistent alignment between observed performance and theoretical calculations highlights the reliability of the EP implementation using GMF, offering a substantial solution to mitigate advanced noise interferences in STAP radar.

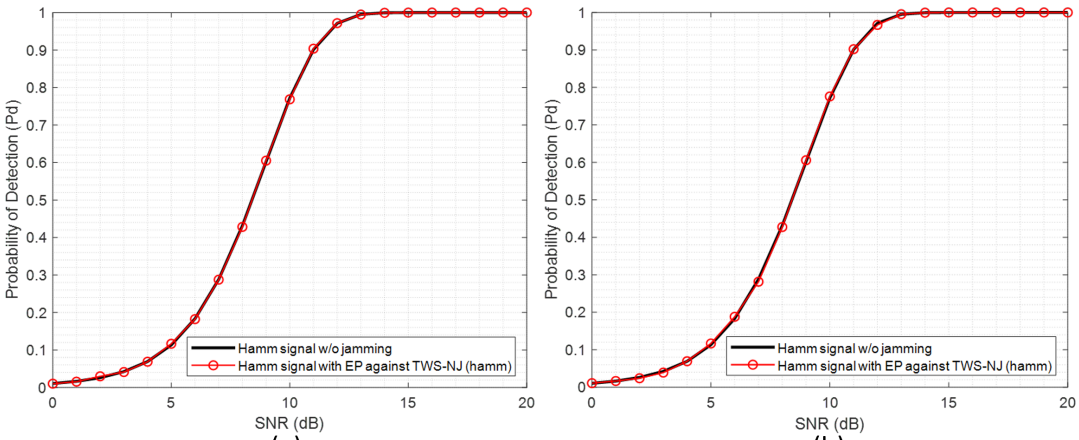

Figure 4.7. P_D vs SNR detection performance curves under EA by TWS-NJ (hamm) with EP implemented. (a) JNR = 5 dB and (b) JNR = 10 dB. Both target and noise interference signals are co-located in spatial cell 9.

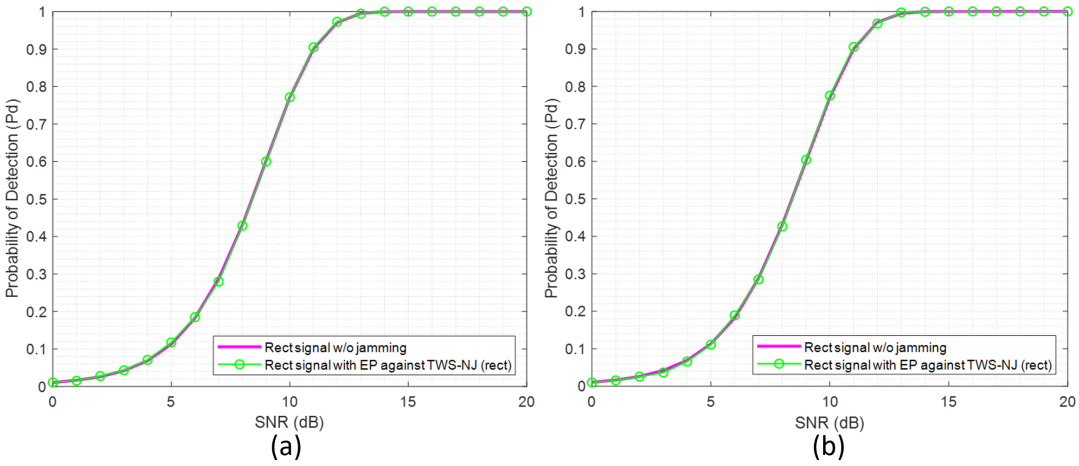

Figure 4.8. P_D vs SNR detection performance curves under EA by TWS-NJ (rect) with EP implemented. (a) JNR = 5dB and (b) JNR = 10 dB. Both target and noise interference signals are co-located in spatial cell 9.

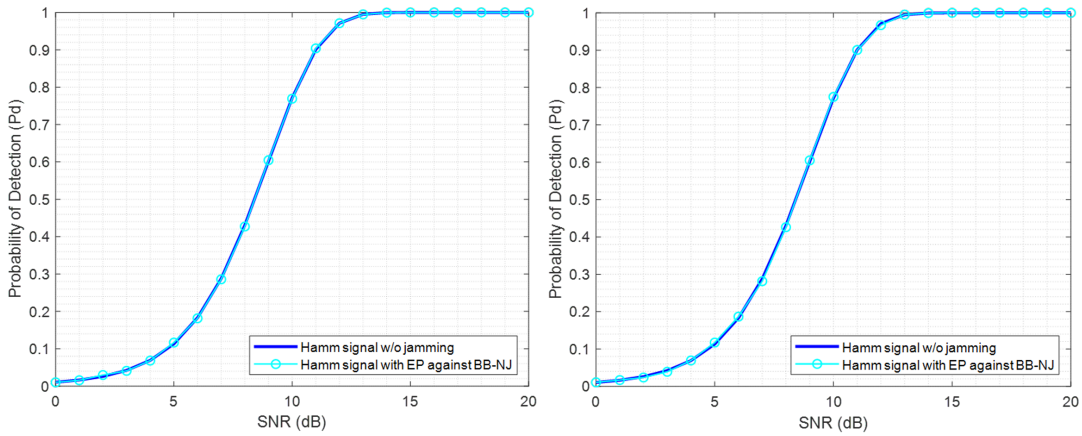

Figure 4.9. P_D vs SNR detection performance curves under EA by BB-NJ with EP implemented. (a) JNR = 5 dB and (b) JNR = 10 dB. Both target and noise interference signals are co-located in spatial cell 9.

4.2.2 Detection Performance for Target and Noise Interference Signals NOT in the same Spatial Cell

Without EP Implementation

In the example illustrated in Fig. 4.10, the target and interference signals are located in spatial cells 9 and 10 respectively. In this case, one can expect that the jamming effect without EP implementation to be reduced when the noise interference is placed away from the target considering the resulting probability of detection curves. It can also be observed that the BB-NJ and TWS-NJ (hamm) have lower impact to degrade detection performance with the JNR value of 5 dB as the P_D curves are relatively close to the performance of the signal not undergoing EA. In Fig. 4.11, a larger JNR value is utilized in order to induce a more pronounced degradation in detection performance.

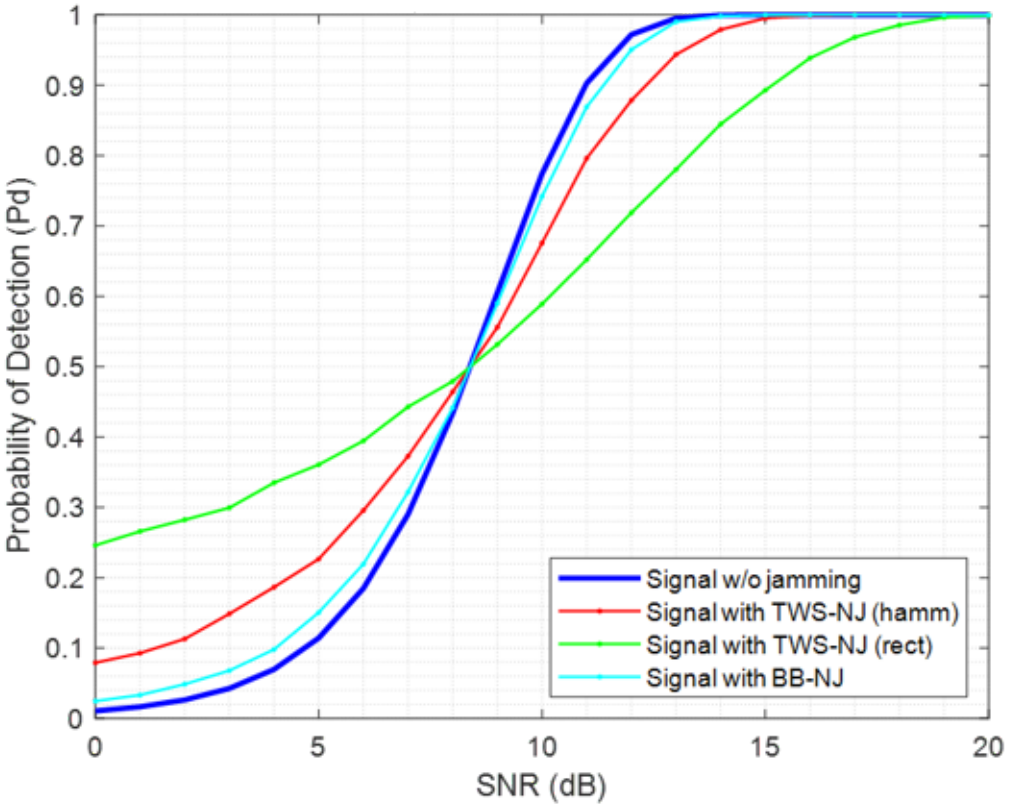

Figure 4.10. P_D vs SNR detection performance curves under EA without EP implemented. JNR = 5 dB. Target and interference signals are located in spatial cells 9 and 10, respectively.

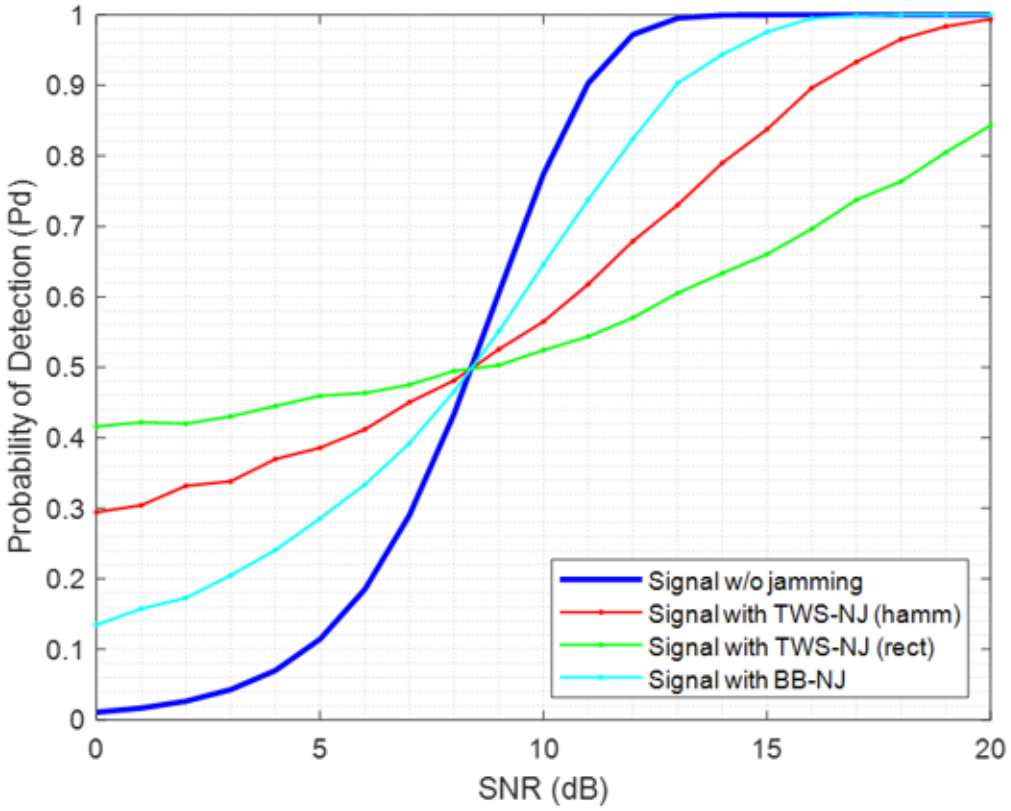

Figure 4.11. P_D vs SNR detection performance curves under EA with EP implemented. JNR = 10 dB. Target and interference signals are located in spatial cells 9 and 10, respectively.

To create the scenario where the noise interference is positioned farther from the target signal, the noise interference is moved farther away to spatial cell 11 while the target signal remained at spatial cell 9. The increase in the spatial distance between the target and the noise interference signal correlates with a diminishing impact on detection performance as illustrated in Fig. 4.12. The observation suggests that to achieve a comparable level of noise interference effectiveness as depicted in Fig. 4.3, a higher JNR of 10 dB is necessary, as illustrated in Fig. 4.13.

This proximity induced amplification highlights the considerations when positioning the noise interference in close proximity to the target, particularly when leveraging the noise interference as a self-protection jammer to assist the target in evading detection.

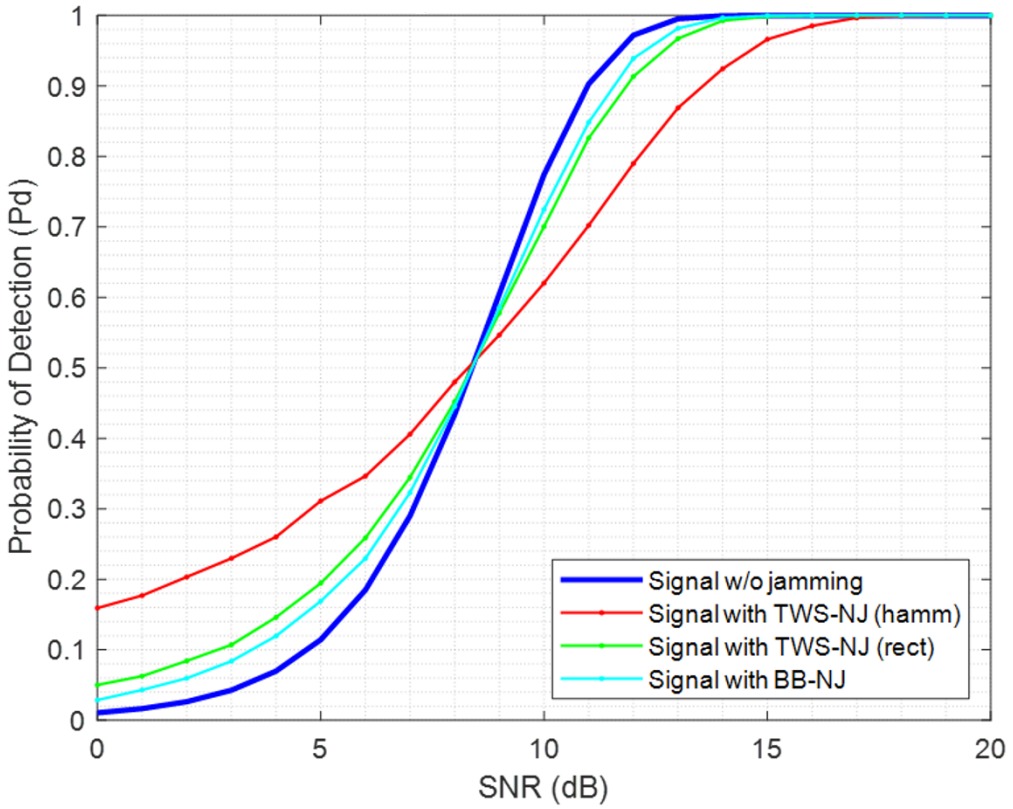

Figure 4.12. P_D vs SNR detection performance curves under EA without EP implemented. JNR = 5 dB. Target and interference signals are located in spatial cells 9 and 11, respectively.

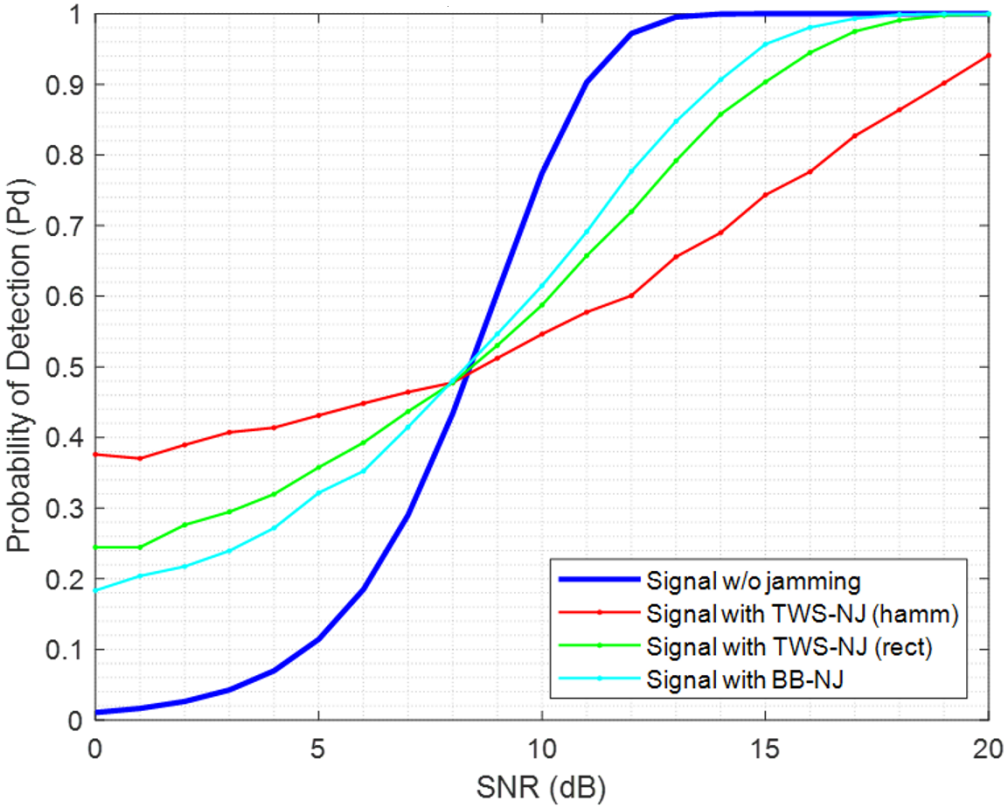

Figure 4.13. P_D vs SNR detection performance curves under EA with EP implemented. JNR = 10 dB. Target and interference signals are located in spatial cells 9 and 11, respectively.

As similarly observed, in terms of EA performance effectiveness, the TWS-NJs are more effective and consistently outperform the BB-NJ in most cases leading to worse degradation of P_D across all JNR values.

With EP Implementation

In line with the previous cases, the implementation of EP consistently yields improvements in detection performance for both the TWS-NJ and the BB-NJ across all JNR values, as illustrated in Fig. 4.14 to Fig. 4.16.

This sustained improvement in detection performance highlights the effectiveness of the GMF in countering the clutter and the TWS-NJs. The GMF achieves this through the adjustments of filter weights, leveraging on the inverse of the overall STAP covariance matrix. By nullifying and suppressing unwanted signals, the GMF ensures that the STAP radar system maintains detection performance very close to the theoretically calculated values.

The adaptability of the GMF not only demonstrates its effectiveness against mitigating TWS-NJs and preserving detection performance. The close alignment between the achieved detection performance and theoretically calculated values highlights the reliability of the GMF as EP for the STAP radar receiver, regardless of the relative proximity of the noise interference to the target signal.

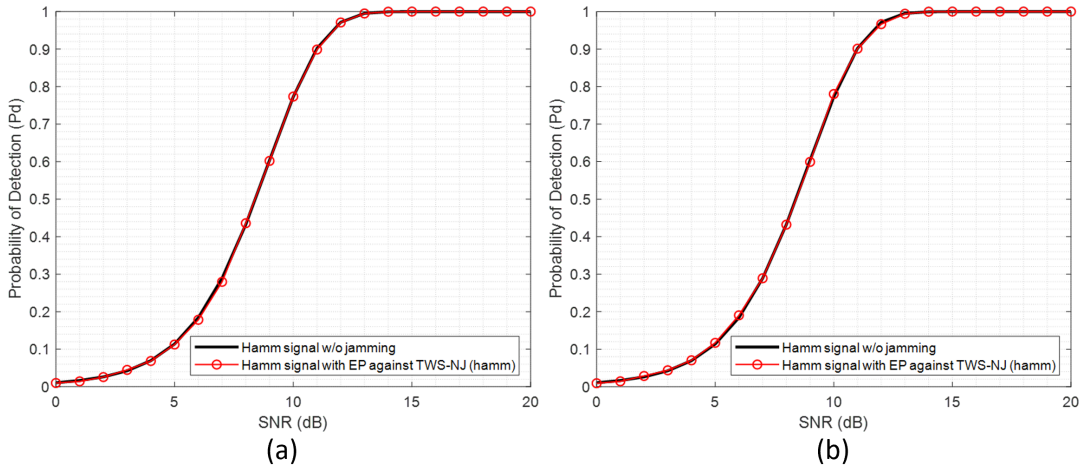

Figure 4.14. P_D vs SNR detection performance curves under EA by TWS-NJ (hamm) with EP implemented. (a) JNR = 5 dB and (b) JNR = 10 dB. Target and interference signals are located in spatial cells 9 and 11, respectively.

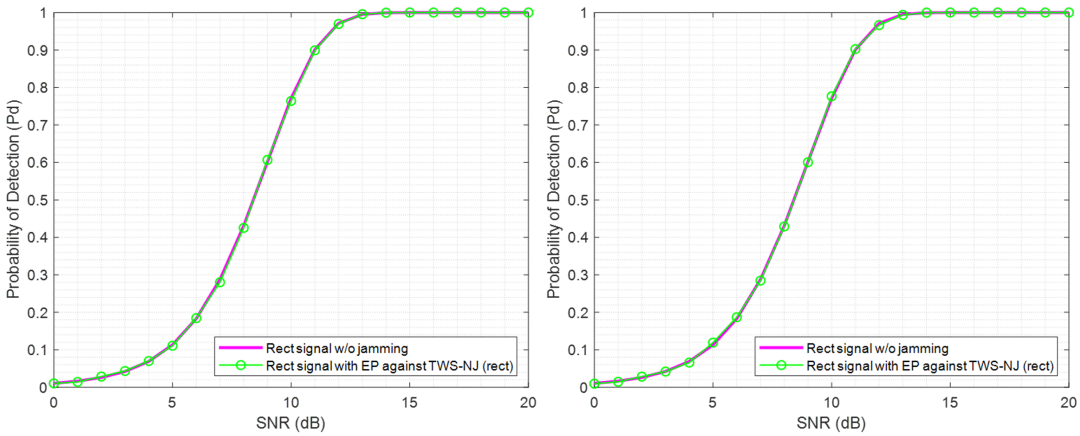

Figure 4.15. P_D vs SNR detection performance curves under EA by TWS-NJ (rect) with EP implemented. (a) JNR = 5 dB and (b) JNR = 10 dB. Target and interference signals are located in spatial cells 9 and 11, respectively.

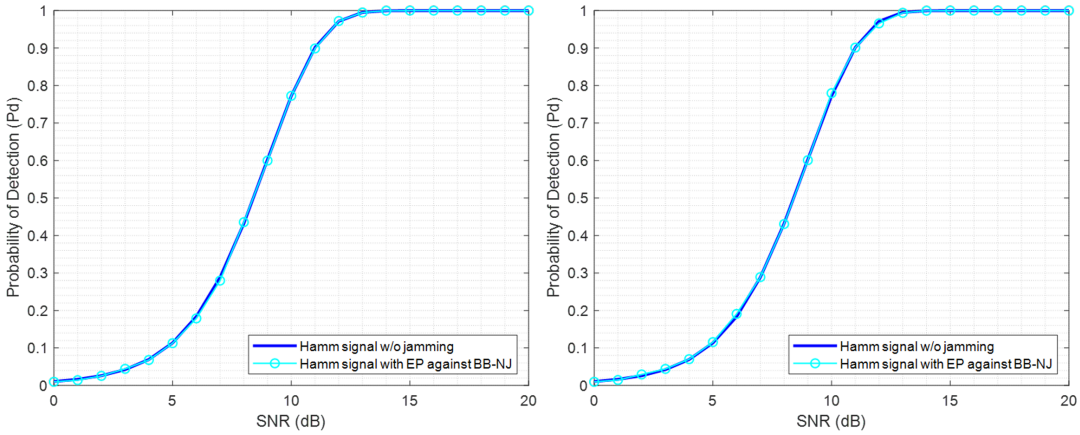

Figure 4.16. P_D vs SNR detection performance curves under EA by BB-NJ with EP implemented. (a) JNR = 5 dB and (b) JNR = 10 dB. Target and interference signals are located in spatial cells 9 and 11, respectively.

THIS PAGE INTENTIONALLY LEFT BLANK

CHAPTER 5:
Conclusion

In this research, we introduced the formulation of the TWS-NJ as an EA into the STAP detection problem and demonstrated its significant impact on target detection, especially when co-located with the target in the same angular cell. The TWS-NJ outperforms the BB-NJ in degrading target detection in most cases when the system is without EP implementation. The observed disparity in interference performance highlights the importance of considering both the waveform characteristics and spatial location of the noise interferences when evaluating their impact on detection performance. We also evaluated that given the required ES support and an accurate estimate of the noise interference covariance matrix, the GMF is a highly effective STAP EP technique to mitigate such adaptive shaped interference.

5.1 Key Findings

5.1.1 Performance of TWS-NJ Against Conventional BB-NJ

As discussed in Chapter 4, it was evident that the TWS-NJ consistently outperforms the conventional BB-NJ in most of the cases, especially at higher JNR values. In addition, along with strategic placement of co-locating the target signal in the same spatial cell, the TWS-NJ is a more effective noise interference, making target detection more challenging for STAP radar receiver.

The superiority of the TWS-NJ over the conventional BB-NJ can be attributed to its waveform shaping technique aimed to exploit the vulnerabilities of the radar signal, creating a more effective interference. By mimicking the frequency characteristics of the radar transmitted waveform, the TWS-NJ posed a greater challenge for the STAP radar receiver without EP implementation to detect signal from noise. This finding underscores the importance of evolving EW tactics and echoes similar findings in [10], which showed the potency of the TWS-NJ in EA.

5.1.2 Impact of Noise Interference Shape in TWS-NJ

The comparison between the TWS-NJ (hamm) and TWS-NJ (rect) reveals subtle performance difference based on angular location. While TWS-NJ (hamm) demonstrates superior noise interference performance in specific spatial cells as observed in Fig. 4.4, the TWS-NJ (rect) otherwise, outperforms the TWS-NJ (hamm) in simulations involving different angles as illustrated in Fig 4.6.

This performance variation highlights the significance of the pulse shape in directing noise interference energy effectively, and to tailor the noise interference characteristics to specific operational scenarios. In scenarios where the target and noise interference are positioned at different angles, the TWS-NJ (rect) might prove to be more effective to disrupt target detection, as it facilitates a more precise concentration of energy in a narrower main beam. This finding therefore underscores the need for a comprehensive understanding of how different noise interference shapes interact with varying angular configurations, guiding the selection of optimal noise interference strategies for specific EW scenarios.

5.1.3 Impact of Spatial Separation of Noise Interference and Target

The simulation results indicate that the impact of noise interference on detection performance diminishes when the target and interference signals are spatially separated. As a result, higher JNR values are required to compensate in order to achieve the same jamming effects.

The observed impact of spatial separation highlights the need for strategic positioning of noise interference sources. When noise interference sources are positioned too far away from the target, the radar system exhibits reduced vulnerability to jamming effects. This finding therefore underscores the importance of considering spatial configurations in EW scenarios, where the tactical positioning of the noise interference becomes essential to maximize interference effectiveness or minimize the risk of detection.

5.1.4 Effectiveness of EP using GMF

The implementation of EP using GMF proves to be highly effective in mitigating interference effects caused by both TWS-NJ and conventional BB-NJ. The adaptability of the GMF to adjust the filter weights via the inverse of the interference covariance matrix contributes to preserving the STAP radar receiver capabilities.

This success has proven the effectiveness of the GMF as an adaptive receiver by leveraging an accurate estimate of the noise interference covariance matrix. Through this approach, the GMF is able to nullify unwanted signals to achieve optimal SINR and thus, significantly enhances detection capabilities. This finding emphasizes the importance of incorporating sopisticated EP methods such as GMF to counter advanced noise interferences.

5.2 Future Research

5.2.1 Optimizing TWS-NJ for Specific Scenarios

One of the future research areas is the optimization of TWS-NJ effect. This can involve a detailed exploration of various transmit waveform shapes and their impact on clutter. In addition, given the observed impact of spatial separation and choice of TWS-NJ waveform shape on detection performance, future research may concentrate on developing a better understanding and exploiting spatial dynamics in radar systems. This involves investigating optimal spatial configurations for noise interference placement to either maximize interference effectiveness or minimize the risk of detection.

5.2.2 Sidelobe Susceptibility to TWS-NJ

Another critical aspect of radar system performance is the behavior of antenna sidelobes when subjected to TWS-NJ effect. Future studies can investigate the vulnerability of antenna sidelobes to noise jamming, and to examine how different TWS-NJ waveform shapes can affect the sidelobe levels. By understanding these effects, research can guide the design of more robust antenna patterns and adaptive filtering techniques to mitigate the adverse impact of TWS-NJ on overall detection capability of a radar receiver.

5.2.3 Real-World Validation and Experimentation

To bridge the gap and validate simulation results and theoretical findings, future research should include real-world experimentation and validation in operational environments. Conducting field trials with actual radar systems under various EW scenarios can provide valuable insights to the proposed interference mitigation techniques thus ensuring the effectiveness and reliability of developed strategies in authentic electronic warfare conditions.

List of References

[1] W.L. Melvin, "A STAP overview," in *IEEE Aerospace and Electronic Systems Magazine*, Edison, NJ, USA, 2004. Available: 10.1109/MAES.2004.1263229.

[2] D. J. O'Donohue, "Joint electromagnetic spectrum operations," vol. 3, no. 85, pp. 1–13, May 2020.

[3] M. von Spreckelsen, "Electronic warefare - The forgottten discipline: Why is the refocus on this traditional warfare area key for modern conflict?" vol. 27, no. 1, pp. 41–45, Dec 2018. Available: https://www.japcc.org/electronic-warfare-the-forgotten-discipline/.

[4] William L. Melvin, James A. Scheer, *Principles of Modern Radar Vol. II: Advanced Techniques*. Edison, NJ, USA: SciTech Publishing, 2013.

[5] J. R. Guerci., *Space-time Adaptive processing for radar*. Boston, MA, USA: Artech House, 2003.

[6] Z. Y. B. Wang, X. Yang and T. Lan, "Dense false-target jamming suppression method by utilizing BI-phase random coded waveform for space time adaptive processing," in *IET International Radar Conference (IET IRC 2020), Online Conference*, 2020. Available: 10.1049/icp.2021.0544.

[7] X. X. Z. Lei, S. Jinping and T. Jihua, "Space-time adaptive processing for sea clutter and jamming suppression in radar seekers," in *2010 2nd International Conference on Signal Processing Systems*, 2010. Available: 10.1109/ICSPS.2010.5555440.

[8] S. P. Chaitra and D. Kumuda, "Target detection using space time adaptive processing," in *2019 4th International Conference on Recent Trends on Electronics, Information, Communication and Technology (RTEICT)*, 2019. Available: 10.1109/RTEICT46194.2019.9016859.

[9] Y. P. C. W. N. Tai, H. Zhu and N. Yuan, "Coherent noise jamming to de-chirping radar," in *015 IEEE International Conference on Signal Processing, Communications and Computing (ICSPCC)*, 2015. Available: 10.1109/ICSPCC.2015.7338805.

[10] A. L. Feltes and R. A. Romero, "Electronic protection mitigation techniques against transmit waveform shaped noise jammers," in *2021 IEEE Radar Conference (RadarConf21)*, 2021. Available: 10.1109/RadarConf2147009.2021.9455292.

[11] Q. J. O. Tan and R. A. Romero, "Jammer-nulling transmit-adaptive radar against knowledge-based jammers in electronic warfare," vol. 7, pp. 181 899–181 915, 2019. Available: 10.1109/ACCESS.2019.2960012.

[12] Kay, S.M., *Fundamentals of Statistical Signal Processing: Detection Theory*. Upper Saddle River, NJ, USA: Prentice Hall, 1998.

Initial Distribution List

1. Defense Technical Information Center
   Ft. Belvoir, Virginia

2. Dudley Knox Library
   Naval Postgraduate School
   Monterey, California